



ELSEVIER

Journal of Alloys and Compounds 275–277 (1998) 407–411

Journal of
ALLOYS
AND COMPOUNDS

The simulation of polarised absorption and magnetic circular dichroism in LiYF₄:Nd³⁺

Hilde de Leebeeck*, Christiane Görller-Walrand

Department of Chemistry, Coordination Chemistry Division, K.U. Leuven, Celestijnenlaan 200F, B-3001 Leuven, Belgium

Abstract

Polarised absorption spectra of the Nd³⁺ ion in a LiYF₄ host are recorded at 4.2 and 150 K and at room temperature in a region of 240–2500 nm. The determination of the CF energy level scheme is completed and labelling of the levels with irreducible representations of the S₄ point group is carried out. The CF wavefunctions are derived using a free-ion and CF hamiltonian which results in the optimisation of 27 parameters. The dipole strengths of the transitions are used to optimise 12 intensity parameters. The free ion, CF and intensity parameters are evaluated by means of the graphical comparison of simulated and experimental spectra. In addition, magnetic circular dichroism of LiYF₄:Nd³⁺ is registered in the region of 257–875 nm at 4.2 K with the magnetic field of 0.9 T along the optical c-axis. The Zeeman levels are analysed using the optimised free ion and CF parameters. The obtained intensity parameter set is then used to calculate the dipole strengths of the transitions between the Zeeman levels. The comparison of simulated and experimental MCD spectra is a test of the value of the optimised parameter sets. © 1998 Elsevier Science S.A.

Keywords: LiYF₄:Nd³⁺; Optics; Magneto-optics; Energy levels; Dipole strength; Magnetic circular dichroism

1. Introduction

In this paper the polarised absorption spectra of LiYF₄:Nd³⁺ are used to optimise 27 parameters to describe the free ion and crystal field perturbations. In addition the dipole strengths of the transitions are used to fit 12 intensity parameters. These parameter sets are sufficient to describe the spectroscopic properties of the neodymium³⁺ ion in a LiYF₄ host. This will be proved in the graphical comparison of the predicted and experimental magnetic circular dichroism of LiYF₄:Nd³⁺.

2. Experimental details

The optical spectra are taken on an oriented LiYF₄ single crystal doped with 1.5% neodymium³⁺.

The polarised absorption spectra are recorded on an AVIV 17 DS spectrophotometer. The optical region of 240–2500 nm is investigated at 4.2 and 150 K and at room temperature using an Oxford 1204 continuous flow cryostat.

The magnetic circular dichroism is registered on an AVIV 62 MCD DS CD spectrophotometer at 4.2 K using

the same cryostat. The optical axis of the LiYF₄:Nd³⁺ complex is positioned along the magnetic field lines of a 9000 G Oxford N177 electromagnet.

3. Discussion

3.1. Simulation of the crystal field energy level scheme

The electronic configuration of neodymium³⁺ (f³) is disturbed by eight fluorine ions in the first coordination sphere of the central rare earth ion. These form a slight distorted dodecahedron with S₄ symmetry [1]. The parametrisation of the energy levels of the neodymium³⁺ ion in a LiYF₄ host are given in Eq. (1) [2,3].

$$\begin{aligned} E = & E_{\text{av}} + \sum_{k=2,4,6} f_k F^k + \zeta_{\text{nl}} A_{\text{SO}} + \alpha L(L+1) + \beta G(G_2) \\ & + \gamma G(R_7) + \sum_{i=2,3,4,6,7,8} T^i t_i + \sum_{k=2,4,6} P^k p_k \\ & + \sum_{k=0,2,4} M^k m_k + B_0^2 C_0^2 + B_0^4 C_0^4 + B_0^6 C_0^6 \\ & + B_4^4 (C_4^4 + C_{-4}^4) + i B_4^4 (C_4^4 + C_{-4}^4) + B_4^6 (C_4^6 + C_{-4}^6) \\ & + i B_4^6 (C_4^6 + C_{-4}^6) \end{aligned} \quad (1)$$

*Corresponding author.

Table 1

Optimised free ion and crystal field parameters (in cm^{-1}) for $\text{LiYF}_4:\text{Nd}^{3+}$

Parameter	Parameter value	Parameter	Parameter value
Central field		Spin–spin and spin-other-orbit	
E_{av}	24 413	M^0	0.7
Electron repulsion		M^2	0.4
F^2	72 911	M^4	0.3
F^4	52 471	Electrostatic correlated SOC	
F^6	35 486	P^2	195
Spin-orbit coupling (SOC)		P^4	146
ζ	872	P^6	98
Two-body interaction		Crystal field S_4	
α	21	B_0^2	372
β	-575	B_0^4	-972
γ	1488	B_0^6	-20
Three-body interaction		B_4^4	-1116
T^2	226	iB_4^4	-599
T^3	43	B_4^6	-1018
T^4	87	iB_4^6	-194
T^6	-285		
T^7	320		
T^8	212		

The parameters which appear in Eq. (1) incorporate the radial parts of the matrix elements $\langle \psi | H | \psi \rangle$ and are optimised [4] using the experimental derived energy levels. The assignment of the energy levels is not only based on the position of the levels [5] but also on the labelling with irreducible representations [6,7]. This labelling is deduced from the selection rules of polarised absorption using group theory for the S_4 point group. In addition the α polarised measurements were found to be similar to the σ polarised measurements.

polarisation, indicating the predominantly electric dipole (ED) character of the transitions.

The combination of the position and labelling of the CF energy levels makes it possible to assign the correct eigenvalue to the observed energy level.

A total of 27 parameters (free ion and crystal field) are optimised together in one diagonalisation fitting to 149 labelled energy levels. The values and significations of the parameters are listed in Table 1 and the calculated energy levels are compared with the experimental labelled levels in Table 2.

It appears that the values for the imaginary parts of the B_4^4 and B_4^6 are of considerable magnitude when the only slight distortion of the dodecahedron (D_{2d}), where the imaginary parts iB_4^4 and iB_4^6 are absent, is taken into account. The values for the iB_4^4 and iB_4^6 are caused by the mixing of the wavefunctions of the neodymium complex when J–J-mixing is allowed. In addition we prefer not to work with an arbitrary choice of the position of the axes [5] but to follow the conventions of Koster et al. [8].

3.2. Simulation of the transition probability

The transition probability in the polarised absorption spectra can be expressed as a dipole strength D . As was concluded earlier the transitions of the neodymium ion in LiYF_4 posses predominantly an electric dipole character. In order to calculate the electric dipoles one needs the wavefunctions of the system and an additional set of

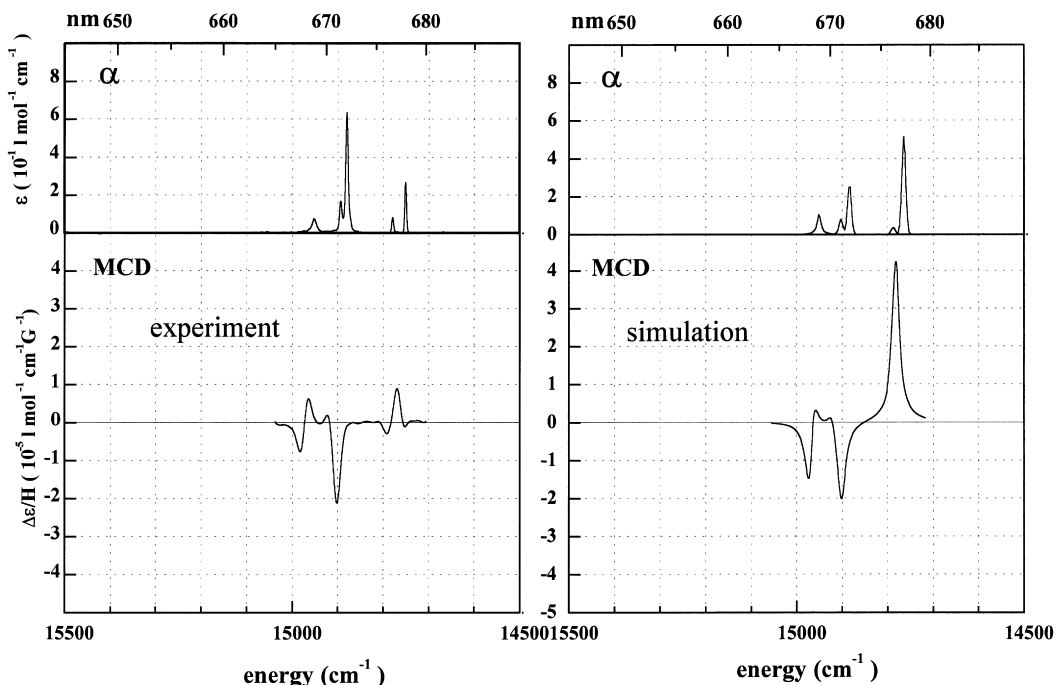


Fig. 1. Comparison of the experimental and simulated ${}^4\text{F}_{9/2} \leftarrow {}^4\text{I}_{9/2}$ transitions in the polarised absorption and magnetic circular dichroism spectra of $\text{LiYF}_4:\text{Nd}^{3+}$.

Table 2

Comparison of the labelled experimental and simulated energy levels (in cm^{-1}) of $\text{LiYF}_4:\text{Nd}^{3+}$ according to the S_4 symmetry

Multiplet	Label	E_{exp}	E_{calc}	Multiplet	Label	E_{exp}	E_{calc}
$^4\text{I}_{9/2}$	$\Gamma_{7,8}$	0	0	$^4\text{G}_{11/2}$	$\Gamma_{7,8}$	21 812	21 826
	$\Gamma_{7,8}$	130	136		$\Gamma_{5,6}$	21 830	21 827
	$\Gamma_{5,6}$	180	190		$\Gamma_{7,8}$	21 902	21 921
	$\Gamma_{5,6}$	247	275		$\Gamma_{5,6}$	21 948	21 958
	$\Gamma_{7,8}$	523	531		$\Gamma_{5,6}$	21 985	22 003
					$\Gamma_{7,8}$	21 994	22 015
					$\Gamma_{7,8}$	23 404	23 415
					$\Gamma_{5,6}$	23 898	23 925
					$\Gamma_{5,6}$	23 942	23 958
					$\Gamma_{5,6}$	24 038	24 026
$^4\text{I}_{11/2}$	$\Gamma_{7,8}$	1988		$^2\text{K}_{15/2}$	$\Gamma_{7,8}$	26 264	26 288
	$\Gamma_{5,6}$	2033			$\Gamma_{5,6}$	26 344	26 339
	$\Gamma_{7,8}$	2036			$\Gamma_{5,6}$	28 110	28 098
	$\Gamma_{5,6}$	2077			$\Gamma_{7,8}$	28 217	28 218
	$\Gamma_{5,6}$	2228			$\Gamma_{5,6}$	28 372	28 371
	$\Gamma_{7,8}$	2266			$\Gamma_{5,6}$	28 529	28 570
	$\Gamma_{5,6}$	3933	3942		$\Gamma_{7,8}$	28 584	28 584
	$\Gamma_{7,8}$	3949	3965		$\Gamma_{7,8}$	28 803	28 814
	$\Gamma_{5,6}$	3993	3990		$\Gamma_{5,6}$	29 206	29 239
	$\Gamma_{7,8}$	4026	4017		$\Gamma_{7,8}$	29 296	29 297
$^4\text{I}_{13/2}$	$\Gamma_{5,6}$	4204	4208	$^4\text{D}_{3/2}$	$\Gamma_{7,8}$	29 377	29 399
	$\Gamma_{5,6}$	4221	4243		$\Gamma_{7,8}$	29 467	29 522
	$\Gamma_{7,8}$	4241	4246		$\Gamma_{5,6}$	29 719	29 694
	$\Gamma_{5,6}$	5854	5868		$\Gamma_{7,8}$	29 734	29 716
	$\Gamma_{5,6}$	5913	5926		$\Gamma_{7,8}$	30 167	
	$\Gamma_{7,8}$	5946	5964		$\Gamma_{5,6}$	30 235	30 280
	$\Gamma_{7,8}$	6026	6037		$\Gamma_{7,8}$	30 292	30 325
	$\Gamma_{7,8}$	6314	6327		$\Gamma_{5,6}$	30 375	30 366
	$\Gamma_{5,6}$	6348	6367		$\Gamma_{7,8}$	30 450	30 410
	$\Gamma_{7,8}$	6392	6402	$^2\text{L}_{15/2}$	$\Gamma_{5,6}$	30 548	30 582
$^4\text{F}_{3/2}$	$\Gamma_{5,6}$	6434	6443		$\Gamma_{7,8}$	30 592	30 592
	$\Gamma_{7,8}$	11 542	11 540		$\Gamma_{5,6}$	30 574	30 606
$^4\text{F}_{5/2}$	$\Gamma_{5,6}$	11 602	11 580		$\Gamma_{7,8}$	30 599	30 654
	$\Gamma_{7,8}$	12 540	12 531		$\Gamma_{5,6}$	30 672	30 728
$^2\text{H}(2)_{9/2}$	$\Gamma_{5,6}$	12 550	12 566	$^4\text{D}_{7/2}$	$\Gamma_{5,6}$	30 720	30 681
	$\Gamma_{5,6}$	12 632	12 675		$\Gamma_{7,8}$	30 758	30 766
	$\Gamma_{7,8}$	12 647	12 636		$\Gamma_{7,8}$	30 898	30 894
	$\Gamma_{5,6}$	12 670	12 690		$\Gamma_{5,6}$	30 925	30 939
	$\Gamma_{7,8}$	12 736	12 791		$\Gamma_{7,8}$	31 062	31 050
	$\Gamma_{5,6}$	12 809	12 806		$\Gamma_{7,8}$	31 060	31 060
	$\Gamma_{7,8}$	12 843	12 881		$\Gamma_{5,6}$	31 645	31 673
	$\Gamma_{7,8}$	13 499	13 516		$\Gamma_{7,8}$	31 743	31 743
	$\Gamma_{5,6}$	13 524	13 533		$\Gamma_{5,6}$	31 800	31 791
	$\Gamma_{7,8}$	13 630	13 643		$\Gamma_{7,8}$	31 858	31 859
$^4\text{F}_{7/2}$	$\Gamma_{7,8}$	13 640	13 660	$^2\text{L}_{17/2}$	$\Gamma_{7,8}$	31 890	31 887
	$\Gamma_{5,6}$	13 650	13 649		$\Gamma_{5,6}$	31 934	31 931
	$\Gamma_{7,8}$	13 662	13 662		$\Gamma_{7,8}$	31 940	31 948
	$\Gamma_{5,6}$	14 753	14 765		$\Gamma_{7,8}$	32 048	32 072
	$\Gamma_{7,8}$	14 783	14 788		$\Gamma_{5,6}$	32 096	32 082
	$\Gamma_{7,8}$	14 882	14 884		$\Gamma_{7,8}$	32 920	32 954
	$\Gamma_{5,6}$	14 896	14 903		$\Gamma_{7,8}$	33 019	33 038
	$\Gamma_{7,8}$	14 954	14 951		$\Gamma_{5,6}$	33 104	33 108
	$\Gamma_{7,8}$	15 928	16 012		$\Gamma_{7,8}$	33 155	33 153
	$\Gamma_{5,6}$	15 976	16 011		$\Gamma_{7,8}$	33 433	33 446
$^2\text{H}(2)_{11/2}$	$\Gamma_{7,8}$	16 002	16 031	$^2\text{H}(1)_{9/2}$	$\Gamma_{7,8}$	33 516	33 529
	$\Gamma_{5,6}$	16 063	16 044		$\Gamma_{5,6}$	34 232	34 250
	$\Gamma_{7,8}$	16 136	16 070		$\Gamma_{7,8}$		
	$\Gamma_{5,6}$	16 147	16 100		$\Gamma_{7,8}$		
	$\Gamma_{7,8}$	17 163	17 185		$\Gamma_{7,8}$		
	$\Gamma_{5,6}$	17 274	17 278		$\Gamma_{7,8}$		
	$\Gamma_{7,8}$	17 301	17 333		$\Gamma_{7,8}$		
	$\Gamma_{5,6}$	17 412	17 404		$\Gamma_{7,8}$		
	$\Gamma_{7,8}$	17 423	17 396		$\Gamma_{5,6}$		
	$\Gamma_{7,8}$	17 479	17 479		$\Gamma_{7,8}$		
$^2\text{G}(1)_{7/2}$	$\Gamma_{5,6}$	17 653	17 668	$^2\text{H}(1)_{11/2}$	$\Gamma_{5,6}$		

Table 2. Continued

Multiplet	Label	E_{exp}	E_{calc}	Multiplet	Label	E_{exp}	E_{calc}
$^4G_{7/2}$	$\Gamma_{7,8}$	19 072	19 042		$\Gamma_{5,6}$	34 289	34 303
	$\Gamma_{5,6}$	19 082	19 081		$\Gamma_{7,8}$	34 333 8	34 310
	$\Gamma_{5,6}$	19 185	19 196		$\Gamma_{5,6}$	34 429	34 436
	$\Gamma_{7,8}$	19 215	19 214		$\Gamma_{7,8}$	34 460	34 437
$^4G_{9/2}$	$\Gamma_{7,8}$	19 464	19 462		$\Gamma_{7,8}$	34 501	
	$\Gamma_{5,6}$	19 564	19 556		$\Gamma_{5,6}$	34 523	34 508
	$\Gamma_{7,8}$	19 618	19 620	$^2D(2)_{5/2}$	$\Gamma_{7,8}$	34 641	
$^2K_{13/2}$	$\Gamma_{5,6}$	19 668	19 668		$\Gamma_{5,6}$	34 644	
	$\Gamma_{5,6}$	19 691	19 711	$^2F(2)_{5/2}$	$\Gamma_{5,6}$	38 458	38 533
	$\Gamma_{7,8}$	19 700	19 702		$\Gamma_{5,6}$	38 672	38 628
$^4G_{9/2}$	$\Gamma_{7,8}$	19 719	19 738		$\Gamma_{7,8}$	38 704	38 693
$^2K_{13/2}$	$\Gamma_{7,8}$	19 727	19 757	$^2F(2)_{7/2}$	$\Gamma_{5,6}$	39 924	39 983
$^4G_{9/2}$	$\Gamma_{5,6}$	19 792	19 742		$\Gamma_{7,8}$	39 970	39 968
$^2K_{13/2}$	$\Gamma_{5,6}$	19 823	19 808		$\Gamma_{5,6}$	40 070	40 051
	$\Gamma_{7,8}$	19 950	19 976		$\Gamma_{7,8}$	40 179	40 143
	$\Gamma_{5,6}$	19 973	19 992	$^2G(2)_{9/2}$	$\Gamma_{7,8}$	48 010	
$^2G(1)_{9/2}$	$\Gamma_{5,6}$		21 020		$\Gamma_{7,8}$	48 121	
	$\Gamma_{7,8}$	21 063	21 054		$\Gamma_{5,6}$	48 138	
	$\Gamma_{5,6}$	21 072	21 091		$\Gamma_{7,8}$	48 235	
	$\Gamma_{7,8}$	21 083	21 098		$\Gamma_{5,6}$	48 262	
$^2D(1)_{3/2}$	$\Gamma_{7,8}$	21 111	21 182	$^2G(2)_{7/2}$	$\Gamma_{7,8}$	48 925	
	$\Gamma_{7,8}$	21 283	21 318		$\Gamma_{5,6}$	49 028	
	$\Gamma_{5,6}$	21 335	21 335		$\Gamma_{7,8}$	49 165	
$^4G_{11/2}$	$\Gamma_{5,6}$	21 440	21 457		$\Gamma_{5,6}$	49 218	
	$\Gamma_{7,8}$	21 462	21 470	$^2F(1)_{7/2}$	$\Gamma_{7,8}$	67 030	
	$\Gamma_{5,6}$	21 555	21 586		$\Gamma_{5,6}$	67 329	
$^2K_{15/2}$	$\Gamma_{5,6}$	21 713	21 688		$\Gamma_{7,8}$	67 566	
	$\Gamma_{7,8}$	21 730	21 721		$\Gamma_{5,6}$	67 595	
	$\Gamma_{5,6}$	21 750	21 754	$^2F(1)_{5/2}$	$\Gamma_{5,6}$	68 309	
	$\Gamma_{7,8}$	21 776	21 785		$\Gamma_{7,8}$	68 739	
	$\Gamma_{7,8}$	21 806	21 818		$\Gamma_{5,6}$	68 767	

intensity parameters $A_{\lambda\text{tp}}$ values which will be optimised [9] using the experimental dipole strengths. The expression of the global dipole strength [10,11] is given in Eq. (2) where χ are the local field corrections. The optimised intensity parameters are given in Table 3.

$$D = \chi_{\text{MD}} \left| \left\langle \psi \mid -\mu_B (L + 2S)^1 \rho \mid \psi' \right\rangle \right|^2 + \chi_{\text{ED}} \cdot e^2 \left[\sum_{\lambda\text{tp}} a_{\lambda\text{tp}} A_{\lambda\text{tp}} \right]^2 \quad (2)$$

3.3. Simulation of the magnetic circular dichroism

The simulation of the magnetic circular dichroism

Table 3
Intensity parameters (in 10^{-12} cm) for $\text{LiYF}_4:\text{Nd}^{3+}$ according to the S_4 symmetry

Parameter	Parameter value
$A_{232} + iA_{232}$	$186 + i263$
$A_{432} + iA_{432}$	$79 + i155$
$A_{452} + iA_{452}$	$-179 + i26$
$A_{652} + iA_{652}$	$-525 - i10$
$A_{672} + iA_{672}$	$228 - i434$
$A_{676} + iA_{676}$	$9 - i14$

requires the Zeeman energy levels and the difference in dipole strengths for left and right circular polarised light.

The Zeeman levels are calculated by means of one diagonalisation introducing the free ion, crystal field and Zeeman perturbations together using the optimised parameter sets.

The dipole strengths for left and right circular polarised light are calculated using the Zeeman wavefunctions and the optimised intensity parameters. The dependence of the optimisation of the parameter sets is clear.

3.4. Graphical comparison of experimental and simulated polarised absorption and magnetic circular dichroism

The graphical simulation is performed using Eq. (3) for the polarised absorption spectra and Eq. (4) for the magnetic circular dichroism [12].

$$\epsilon(\bar{\nu}_{\text{CF}}, T) = 327 \bar{\nu}_{\text{CF}} \frac{X_a(T)}{g_a} D_{\text{calc}} f_{\text{CF}}(\bar{\nu}) \quad (3)$$

$$\frac{\Delta \epsilon(\bar{\nu}_{\text{Zeeman}}, T)}{H} = \frac{327 \bar{\nu}_{\text{Zeeman}} X_a(T) (D_{\text{calc}}^1 - D_{\text{calc}}^r) f_{\text{Zeeman}}(\bar{\nu})}{H} \quad (4)$$

with: ϵ , extinction coefficient ($1 \text{ mol}^{-1} \text{ cm}^{-1}$); $\bar{\nu}$, position of the crystal field (CF) or Zeeman transition (cm^{-1}); T , temperature (K); H , magnetic field (G); X_a , population of the ground field level; g_a , degeneration of the ground field level; D_{calc} , calculated dipole strength (Debye 2); $f(\bar{\nu})$, form function (Lorentz or Gauss).

These graphical simulations are carried out for the complete optical region. We present here (Fig. 1) the ${}^4F_{9/2} \leftarrow {}^4I_{9/2} {}^{3+}$ transitions [12] which illustrate the neodymium ${}^{3+}$ spectra in a single crystalline state. The bands are very narrow and the transitions are not well separated with an overlap of the bands.

4. Conclusions

In this paper the optimisation of the free ion, crystal field and intensity parameters of $\text{LiYF}_4:\text{Nd}^{3+}$ is carried out and evaluated by means of a graphic comparison between the simulated and experimental data. Not only are the used experimental polarised absorption spectra to optimise the parameters compared but, also, another phenomenon can be predicted: magnetic circular dichroism. The position of the transitions is very well predicted, and the comparison of the intensity of the transitions is satisfying.

This shows the independence of the parameter sets of one technique, and proves its value in predicting other properties.

Acknowledgements

We thank M.F. Reid for the disposition of the programs that are used for the optimisations. This work was also financially supported through a grant from the IWONL.

References

- [1] Vishwamittar, S.P. Puri, J. Phys. C Solid State 7 (1974) 1337.
- [2] H.M. Crosswhite, H. Crosswhite, J. Opt. Soc. Am. B1 (1984) 246.
- [3] C. Görller-Walrand, K. Binnemans, Rationalisation of crystal field parametrisation, in: Handbook on the Physics and Chemistry of Rare Earths, North-Holland, Amsterdam, 1997.
- [4] H. de Leebeeck, C. Görller-Walrand, J. Alloy Compounds 225 (1995) 75.
- [5] M.A. Couto dos Santos, P. Porcher, J.C. Krupa, J.Y. Gesland, J. Phys. Condens. Matter 8(25) (1996) 4643.
- [6] A.A.S. da Gama, G.F. de Sa, P. Porcher, P. Caro, J. Chem. Phys. 75(6) (1981) 2583.
- [7] Z. Song, S. Lian, D. Ma, Y. Xu, Y. Gu, Y. Gui, D. Hua, S. Wang, Guangpuxue Yu Guangpu Fenxi 4(5) (1984) 1.
- [8] G.F. Koster, J.O. Dimmock, R.G. Wheeler, H. Statz, Properties of the Thirty-two Point Groups, MIT Press, Cambridge MA, 1993.
- [9] C. Görller-Walrand, L. Fluyt, P. Porcher, A.A.S. da Gama, G.F. de Sa, W.T. Carnall, G.L. Goodman, J. Less-Common Metals 148 (1989) 339.
- [10] C. Görller-Walrand, L. Fluyt, A. Ceulemans, W.T. Carnall, J. Chem. Phys. 95 (1991) 3099.
- [11] M.F. Reid, F.S. Richardson, J. Chem. Phys. 179 (1983) 5735.
- [12] L. Fluyt, E. Hens, H. de Leebeeck, C. Görller-Walrand, J. Alloy Compounds (in press).